A Multistate Frequency Reconfigurable Monopole Antenna Using Fluidic Channels

Aditya Singh, Ian Goode, and Carlos E. Saavedra

***Abstract*—A reconfigurable microstrip monopole antenna that uses three closely spaced substrate milled channels filled with either air or dielectric fluid is presented. Based on the number of channels filled with fluid, four states—namely states 0, 1, 2, and 3—of operation are selected. Introduction of fluid (distilled water) in the channel modifies the effective permittivity of the dielectric medium and perturbs the E-field distribution in vicinity to the antenna arm. The position and size of channels are optimized to maximize the shift in operating frequency and $S_{11} < -10$ dB impedance bandwidth through full-wave electromagnetic (HFSS) simulations. A prototype of the antenna is fabricated and measured, exhibiting frequency shifts of 12.0%, 17.9%, and 23.7% with impedance bandwidth of 32.0%, 30.1%, and 29.9% in states 1, 2, and 3 of the antenna, respectively. The reference state, i.e., state 0, offers 34.7% impedance bandwidth. The measured peak gains achieved are 2.4, 1.6, 1.2, and 0.3 dBi for states 0, 1, 2, and 3, respectively. In all the states of operation, the radiation pattern remains stable and omnidirectional.**

***Index Terms*—Antennas, dielectric fluid, distilled water, frequency tuning, high-power, microfluidics, microstrip monopole, microwaves, reconfigurable, tunable, wearables.**

I. Introduction

RECONFIGURABLE antennas are envisioned as one of the key components in realizing modern-day wireless links for applications such as cognitive radio [1]. Efficient utilization of available spectrum calls for tunable microwave front ends to sense the communication channel and switch to available frequency band [2]. The use of fluids in microwave components and antennas for tuning and reconfigurability has sparked wide interest because of their compatibility with wearable electronics, their power handling capability, low-noise behavior, and their long lifespan compared to microelectromechanical system techniques [3], [4]. Numerous recent works have employed liquid metal such as mercury and eutectic gallium indium alloy (EGaIn) to design antennas with reconfigurability in frequency [5]–[7], polarization [8]–[10], and radiation pattern [11]. Liquid metal can serve applications demanding flexibility, high average power, and linearity requirements. However, liquid-metal-based designs face critical challenge in antenna integration and suffer from problems like stiction and leftover metal oxidation. Different types of treatments are required to overcome these issues, which is an active area of research [12], [13]. An alternative way for tuning planar antennas consists of using dielectric fluids to alter antenna characteristics. Typically, fluids are selected based on dielectric constant and loss tangent. Various combinations of antenna geometry and fluids have been explored. In [14], slot antenna with microfluidic channels patterned on polydimethylsiloxane is proposed. Liquid dielectric contained in the channels is used to perturb the **E**-field on a slot antenna resulting in frequency tuning but with a narrow bandwidth, low efficiency, and need for different types of fluids to realize variable effective permittivity for tuning. A microfluidic cavity placed on top of the radiating edge of a coplanar patch antenna and injected with ethanol, hexanol, and water is reported in [15]. A maximum frequency shift of ~13% is observed when loaded with water. Furthermore, some nonplanar designs have also been proposed. A flexible membrane-based cavity is enclosed below the antenna and pumped with ethyl acetate in [16] to achieve continuous frequency tuning with best simulated efficiency of 69% and 6.8% bandwidth. Moreover, a hybrid layer with tunable height ratio of air to liquid is used as substrate below a patch in [17]. It employs low-loss transformer oil to extract better efficiency with continuous tunable frequency range with limitation of being nonplanar. Water has also been employed to provide radiation pattern reconfiguration [18] and polarization reconfiguration as in [19]. Recently in [20], a wideband microstrip monopole water-loaded antenna with a water-filled channel for frequency switching is presented. However, only two states are available for operation of the antenna.

In this letter, a microstrip-fed monopole antenna with three substrate milled channels orthogonal to length of monopole is proposed. Distilled water filled in the channels is used to modify the effective permittivity and to perturb the **E**-field distribution beneath the monopole arm, resulting in frequency reconfigurability with good tuning range and efficiency.

II. Fluidic Antenna Design

Fig. 1 shows a diagram of the proposed monopole antenna and the backside fluidic channels, including the design parameters and dimensions. The basic monopole follows the structure in [21], but here it has been redesigned for a 1.52 mm thick Rogers-4003 substrate ($\epsilon_r = 3.38$, $\tan\delta = 0.0027$) to radiate at around 5.6 GHz with a 35.5% -10 dB impedance bandwidth (IBW). The length of the monopole arm is set to $\lambda_g/4$, where λ_g is the guided wavelength in microstrip environment [22]. The bottom metal layer serves as the ground plane for the feedline

Manuscript received February 8, 2019; accepted March 4, 2019. Date of publication March 8, 2019; date of current version May 3, 2019. This work was supported in part by a grant from the Natural Sciences and Engineering Research Council of Canada (NSERC). The work of A. Singh was supported in part by the Trillium Scholarship from the Government of Ontario. The work of I. Goode was supported in part by the Ontario Graduate Scholarship. *(Corresponding author: Aditya Singh.)*

The authors are with Department of Electrical and Computer Engineering, Queen's University, Kingston, ON K7L 3N6, Canada (e-mail: singh.aditya@queensu.ca; ian.goode@queensu.ca; saavedra@queensu.ca).

Digital Object Identifier 10.1109/LAWP.2019.2903781

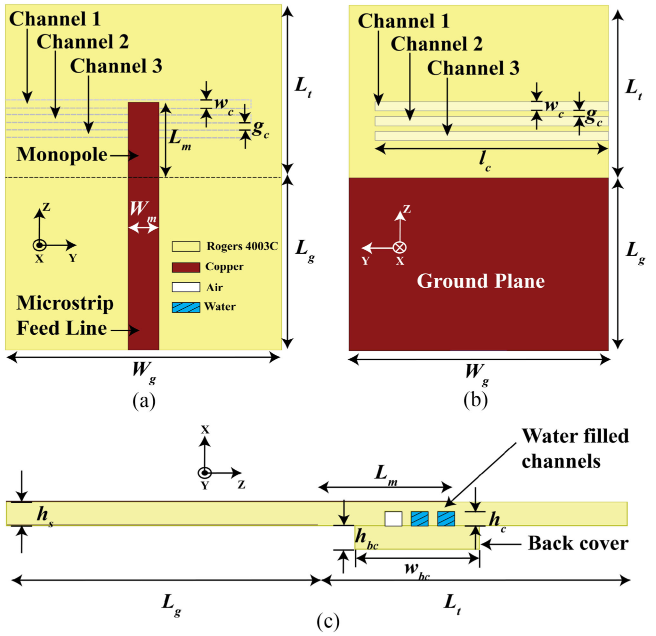

Fig. 1. Microstrip monopole antenna. (a) Front view (dashed lines show channels on back side). (b) Back view without back cover. (c) Cross-sectional view in state 2: $L_g = 20$ mm, $L_t = 20$ mm, $L_m = 8.7$ mm, $W_g = 30$ mm, $W_m = 3.2$ mm, $h_{bc} = 1.52$ mm, $w_{bc} = 10$ mm, $h_s = 1.52$ mm, $l_g = 4$ mm, $g_c = 0.64$ mm, $l_c = 27$ mm, $h_c = 1.0$ mm, and $w_c = 1.08$ mm.

and monopole. The ground plane size and arm width are optimized for the best IBW in state 0 through simulations on ANSYS HFSS. Ground plane size was further optimized and chosen as ($0.61\lambda_g \times 0.92\lambda_g$ at 5.5 GHz) to achieve an omnidirectional radiation pattern [21] and compact size.

For fluidic tuning, three open channels were created on the back side of the antenna by partially milling out the substrate beneath the monopole arm as shown in Fig. 1(b). Another piece of the same substrate is attached to the back side of the antenna using a hot-melt glue gun to create cuboid-shaped closed channels. As a result, one end of each channel remains open to be used as an inlet/outlet port as shown in Fig. 1(c). The width of the channel and the gap between the channels have been intentionally chosen to optimize the frequency shift and allow for in-house fabrication with an LPKF ProtoMat circuit plotter.

The antenna's resonance around $\lambda_g/4$ shifts slightly downwards when the substrate material below the monopole arm is removed to simulate air-filled channels. Since another substrate of the same thickness is added on the back side, this results in downward resonance shift as the effective permittivity exhibited due to combined effect of two substrates and air may be higher. For reconfigurability, the air channels are filled with distilled water. The dielectric constant and loss tangent for water are modeled by using the experimentally verified data ($\epsilon_r \sim 74.6$ and $\tan\delta \sim 0.12$ at 3 GHz) from [23] with piecewise linear interpolation between the frequency range of interest. This introduces discontinuities in the modified medium owing to high relative permittivity of distilled water. Water-filled channels perturb the **E**-field distribution around the monopole arm exhibiting higher effective permittivity of the modified medium. Thus, the $\lambda_g/4$ resonance of the antenna shifts to a lower frequency. Since there are multiple channels, multiple reconfiguration states are

TABLE I
RECONFIGURATION STATES FOR THE ANTENNA

State	Channel 1	Channel 2	Channel 3
0	air	air	air
1	water	air	air
2	water	water	air
3	water	water	water

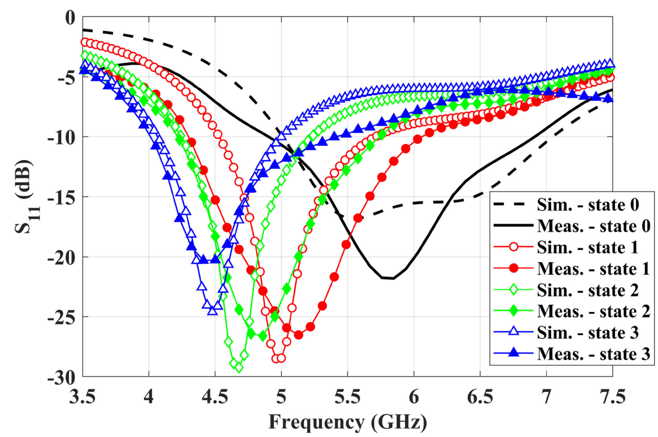

Fig. 2. Measured and simulated S_{11} response for different operating states.

possible. Table I shows the four operating states selected for the antenna. In state 0, all the channels are vacant, and states 1–3 correspond to the configuration when channels are filled with water from the tip of the monopole towards the ground plane (i.e., channels 1–3). A total of seven operating states for the antenna are possible if all (${}^3C_1 + {}^3C_2 + {}^3C_3$, where ${}^nC_k$ denotes n choose k) combinations for filling three available channels with water are considered, where either one, two, or three channel(s) are filled. However, based on considerable performance change from one state to another, only four operating states are selected.

III. RESULTS AND DISCUSSION

The fabricated prototype of the antenna is shown in the inset of Fig. 3. A syringe was used to fill the channel with water, and ports were closed with adhesive tape to retain the water. The antenna's S_{11} response for different operating states defined in Section I is shown in Fig. 2. Overall, a good match is observed for S_{11} response of the antenna showing a close correlation between the simulated and measured response. When all the channels are vacant (filled with air), the simulated center frequency considered at the minimum S_{11} value is 5.52 GHz. Also, the -10 dB IBW in state 0 is $\sim$2.04 GHz (36.9%) where the percentage bandwidth is calculated with respect to center frequency. In state 1, when the channel closest to monopole tip is filled with distilled water, antenna operation shifts to center frequency of 4.98 GHz with IBW of $\sim$1.16 GHz (23.3%). Furthermore, when switched to state 2, since more volume of the substrate is replaced by water, the center frequency shifts further downwards to 4.67 GHz, and IBW is $\sim$0.97 GHz (20.7%). The simulated center frequency in state 3 is found to be 4.48 GHz offering a maximum frequency shift of $\sim$20.7%.

The simulated IBW drops as states change from 0 through 3; this can be attributed to the discontinuity introduced in permittivity of the medium due to the water-filled channel. As the

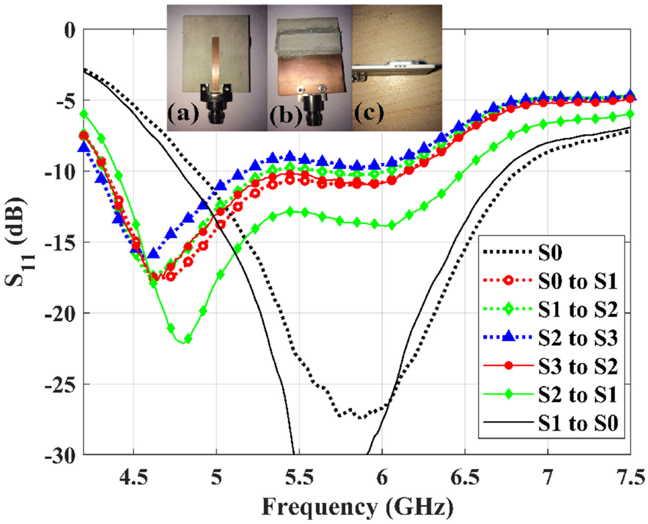

Fig. 3. Measured S_{11} hysteresis and antenna prototype (inset). (a) Front view. (b) Back view (showing glued back cover). (c) Side view (showing vacant channels).

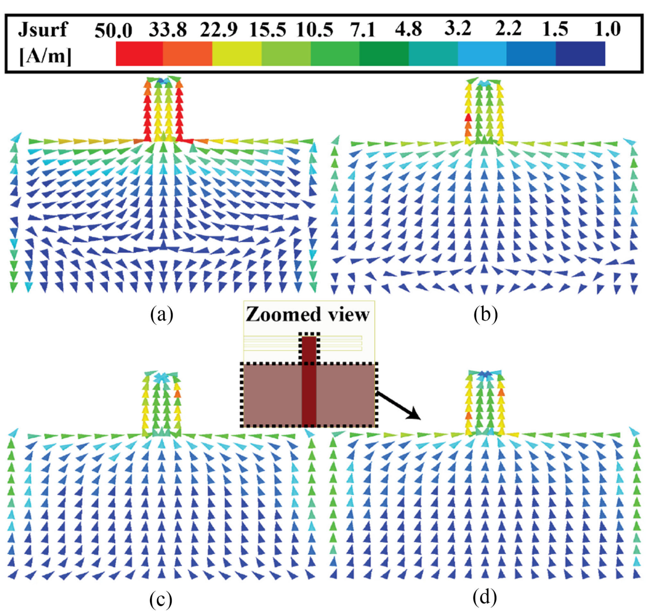

Fig. 4. Surface current distribution on monopole. (a) State 0 (5.5 GHz). (b) State 1 (5 GHz). (c) State 2 (4.7 GHz). (d) State 3 (4.5 GHz).

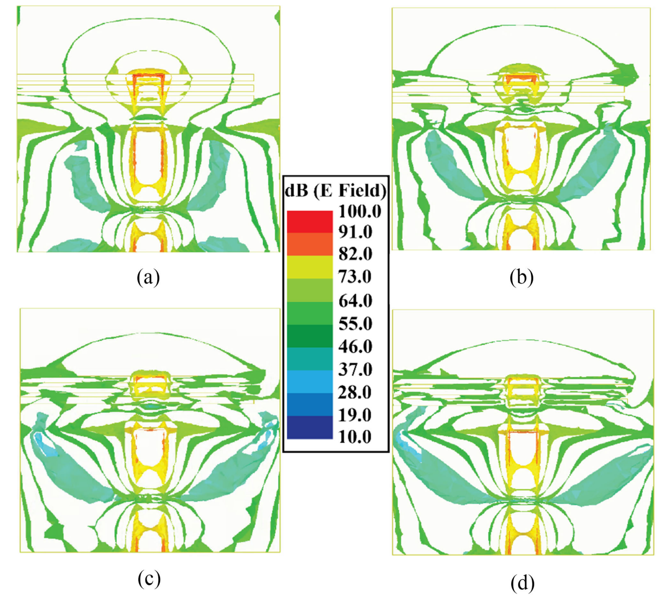

Fig. 5. **E**-field distribution on antenna substrate. (a) State 0 (5.5 GHz). (b) State 1 (5 GHz). (c) State 2 (4.7 GHz). (d) State 3 (4.5 GHz).

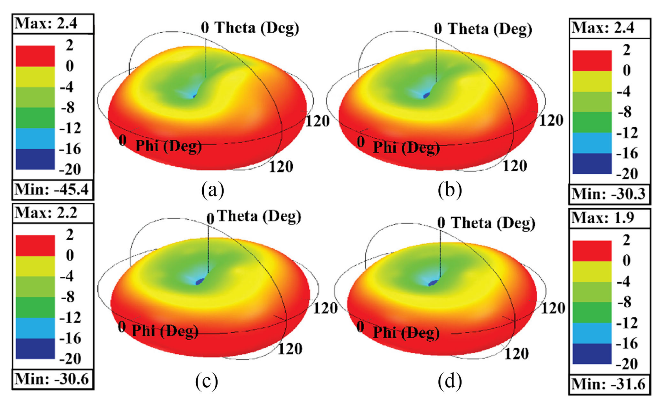

Fig. 6. Realized gain and 3-D radiation pattern. (a) State 0 (5.5 GHz). (b) State 1 (5 GHz). (c) State 2 (4.7 GHz). (d) State 3 (4.5 GHz).

TABLE II
SUMMARY OF ANTENNA PERFORMANCE

Ant. State	Center Freq. (GHz)		IBW (%)		Freq. Shift (%)		Gain (dBi)		Effi. (%)
	sim.	meas.	sim.	meas.	sim.	meas.	sim.	meas.	sim.
0	5.52	5.82	36.9	34.7	-	-	2.4	2.4	97.9
1	4.98	5.12	23.3	32.0	9.8	12.0	2.4	1.6	93.7
2	4.67	4.78	20.7	30.1	15.4	17.9	2.2	1.2	91.7
3	4.48	4.44	20.7	29.9	18.8	23.7	1.9	0.3	90.4

quantity of water increases, it results in higher local effective permittivity. This presents more discontinuity and adversely affects the IBW. Therefore, the IBW in state 0 is deliberately kept large to keep IBW around 20% in lower bands. The differences in IBWs seen in the measured and simulated results can be attributed to fabrication tolerances for the channels, deviation from modeled losses and profile of distilled water inside the channel, and mismatches caused by the glue used in assembly. In the above experiments, the channels were dried with forced air before more water was added. To ascertain the effect of residual water in the channels on S_{11} without drying, a hysteresis analysis was done, and the results are plotted in Fig. 3. The S_{11} responses for all states are reasonably reinstated as the antenna undergoes state change from state 0 to 3 and back from state 3 to 0. However, the resonant frequency and the IBW do change compared to Fig. 2 due to the water residue, which confirms that pumping air through the channels to remove the water is the preferred approach.

The surface current distribution on the antenna and **E**-field distribution (on substrate) are plotted in Figs. 4 and 5 to understand the behavior of the antenna in different operating states. It is observed that with introduction of water into each channel, the electric field tends to concentrate near the channel, and the

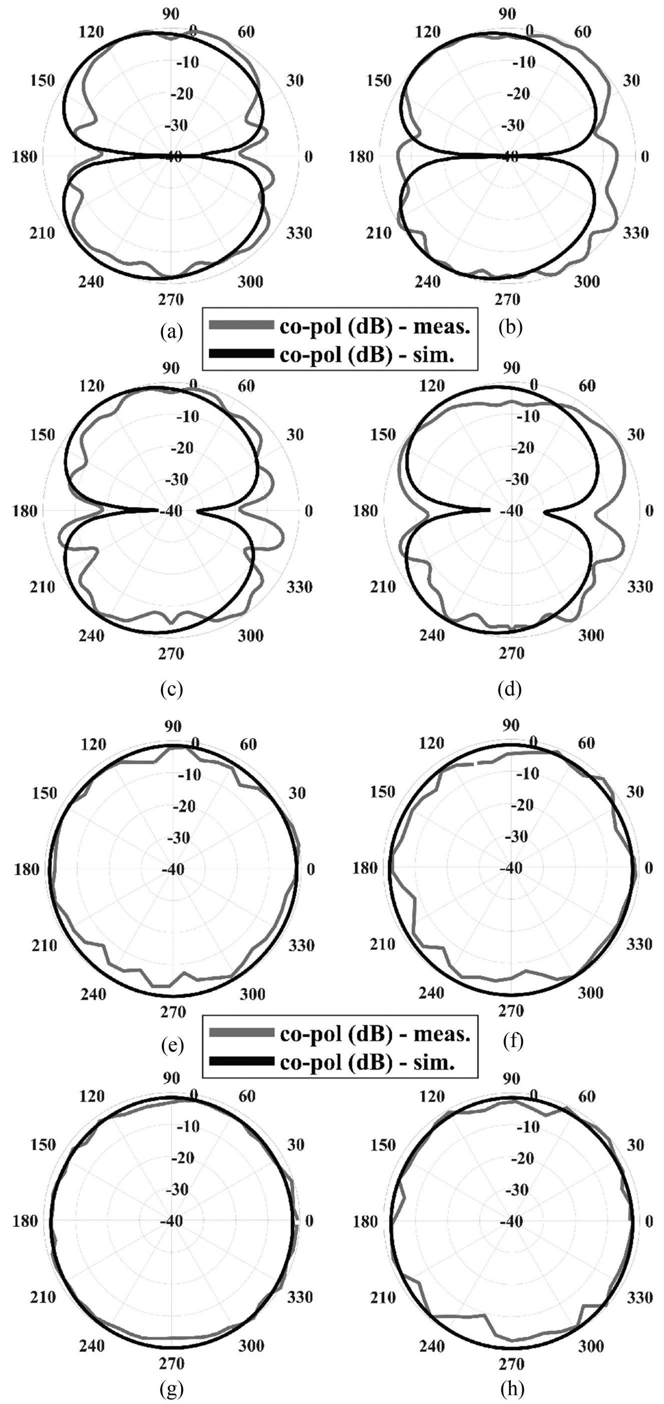

Fig. 7. Measured and simulated radiation patterns in E-plane (*yz*). (a) State 0 (5.5 GHz). (b) State 1 (5 GHz). (c) State 2 (4.7 GHz). (d) State 3 (4.5 GHz) and H-plane (*xy*). (e) State 0 (5.5 GHz). (f) State 1 (5 GHz). (g) State 2 (4.7 GHz). (h) State 3 (4.5 GHz).

TABLE III
COMPARISON WITH REPORTED FREQUENCY-RECONFIGURABLE ANTENNAS

Ref.	Fluid (Antenna type)	Planar	Min. IBW	Tuning (GHz)	Sim. Effi.
[14]	water (slot)	yes	7.5%	7.88-5.44	16%
[15]	water (patch)	yes	13%	3.40-3.80	-
[16]	ethyl acetate (dipole)	No	5%	0.90 -1.44	69%
[17]	transformer oil (patch)	No	5.3%	1.49-1.90	87%
This	water (monopole)	yes	29.9%	5.52-4.48	90.4%

magnitude reduces near the open end of the monopole arm. The current distribution in each state is identical, with dominant current component on the monopole arm, while the ground-plane edge currents cancel due to opposite polarity along horizontal edges and consolidate antenna currents along vertical edges. The 3-D realized gain plots for the antenna are shown in Fig. 6 with a gain of 2.4 dBi in state 0 pertaining to all channels vacant case. However, as the state of operation is switched, the minimum simulated gain is 1.9 dBi in state 3, while the maximum is observed in states 0 and 1 at 2.4 dBi. All the states exhibit ominidirectional radiation pattern identical to basic monopolar radiation pattern. This is due to minimal effect of water-filled channels on the current distribution on the antenna as shown in Fig. 5, resulting in similar far-field behavior. Thus, the reconfiguration methodology can maintain stable radiation pattern and gain when the operating frequency changes in respective state of operation. The minimum simulated radiation efficiency is 90.4% in state 3, while states 0, 1, and 2 are better at 97.9%, 93.7%, and 91.7%, respectively.

Normalized far-field radiation patterns on the principal planes are shown in Fig. 7 for all operating states where E-plane is *yz* and the H-plane is *xy*. To characterize the prototype antenna radiation, measurements were done in the anechoic chamber. The measured results in all the states show omnidirectional pattern correlating with simulated patterns. Furthermore, the measured realized maximum gain was calculated using the Friis transmission formula and shown in Table II. The deviation in measured gain in states 1–3 may be due to higher losses in water compared to modeled values.

IV. CONCLUSION

A multistate operable microstrip-fed monopole antenna has been proposed. The antenna works in four states with stable radiation pattern and gain while showing frequency reconfigurability. Since distilled water is used for reconfiguration, the frequency shift is achieved through modification of effective permittivity while maintaining identical current distribution on the antenna in all states. Thus, radiation patterns are identical in all the states, being omnidirectional. The antenna shows a minimum (state 3) simulated realized gain of 1.9 dBi and efficiency of 90.4%. A comparison with similar reported works has been presented in Table III. In the fluidic planar antenna category, the proposed design offers best-in-class IBW, tuning range, and efficiency. Hysteresis analysis revealed that with injection, the retention of water in channel leads to a downward offset frequency. Therefore, to overcome this issue, the authors aim to include micropumps to clean channel with pressurized air in the future. Also, the aim would be to reduce the design time with initial estimates of channel design parameters through an equivalent circuit model for channel for a desired frequency shift.

ACKNOWLEDGMENT

The authors thank Dr. A. Arbelaez-Nieto for useful discussions on measurements.

REFERENCES

[1] J. Costantine, Y. Tawk, S. E. Barbin, and C. G. Christodoulou, "Reconfigurable antennas: Design and applications," *Proc. IEEE*, vol. 103, no. 3, pp. 424–437, Mar. 2015.

[2] Y. Tawk, J. Costantine, and C. G. Christodoulou, "Cognitive-radio and antenna functionalities: A tutorial [Wireless Corner]," *IEEE Antennas Propag. Mag.*, vol. 56, no. 1, pp. 231–243, Feb. 2014.

[3] K. Entesari and A. P. Saghati, "Fluidics in microwave components," *IEEE Microw. Mag.*, vol. 17, no. 6, pp. 50–75, Jun. 2016.

[4] M. Abdallah and C. E. Saavedra, "Fluidically-tuned reflection oscillator at C-band," in *Proc. Int. Symp. Antenna Technol. Appl. Electromagn. (ANTEM)*, Waterloo, ON, Canada, Aug. 2018, pp. 1–2.

[5] A. Dey, R. Guldiken, and G. Mumcu, "Wideband frequency tunable liquid metal monopole antenna," in *Proc. IEEE Antennas Propag. Soc. Int. Symp.*, Orlando, FL, USA, Jul. 2013, pp. 392–393.

[6] A. J. King, J. F. Patrick, N. R. Sottos, S. R. White, G. H. Huff, and J. T. Bernhard, "Microfluidically switched frequency-reconfigurable slot antennas," *IEEE Antennas Wireless Propag. Lett.*, vol. 12, pp. 828–831, 2013.

[7] S. Shah and S. Lim, "Microfluidically frequency-reconfigurable quasi-Yagi dipole antenna," *Sensors*, vol. 18, no. 9, pii: E2935, 2018.

[8] A. H. Naqvi and S. Lim, "Microfluidically polarization-switchable metasurfaced antenna," *IEEE Antennas Wireless Propag. Lett.*, vol. 17, no. 12, pp. 2255–2259, Dec. 2018.

[9] C. Wang, J. C. Yeo, H. Chu, C. T. Lim, and Y. Guo, "Design of a reconfigurable patch antenna using the movement of liquid metal," *IEEE Antennas Wireless Propag. Lett.*, vol. 17, no. 6, pp. 974–977, Jun. 2018.

[10] M. Wang, M. R. Khan, M. D. Dickey, and J. J. Adams, "A compound frequency and polarization-reconfigurable crossed dipole using multidirectional spreading of liquid metal," *IEEE Antennas Wireless Propag. Lett.*, vol. 16, pp. 79–82, 2017.

[11] D. Rodrigo, L. Jofre, and B. A. Cetiner, "Circular beam-steering reconfigurable antenna with liquid metal parasitics," *IEEE Trans. Antennas Propag.*, vol. 60, no. 4, pp. 1796–1802, Apr. 2012.

[12] J. Lee and C.-J. Kim, "Surface-tension-driven microactuation based on continuous electrowetting," *J. Microelectromech. Syst.*, vol. 9, no. 2, pp. 171–180, Jun. 2000.

[13] Z. Wan, H. Zeng, and A. Feinerman, "Reversible electrowetting of liquid-metal droplet," *J. Fluids Eng.*, vol. 129, no. 4, pp. 388–394, 2006.

[14] C. Murray and R. R. Franklin, "Independently tunable annular slot antenna resonant frequencies using fluids," *IEEE Antennas Wireless Propag. Lett.*, vol. 13, pp. 1449–1452, 2014.

[15] W. Su, B. Cook, M. Tentzeris, C. Mariotti, and L. Roselli, "A novel inkjet-printed microfluidic tunable coplanar patch antenna," in *Proc. IEEE Antennas Propag. Soc. Int. Symp. (APSURSI)*, Memphis, TN, USA, Jul. 2014, pp. 858–859.

[16] M. Konca and P. A. Warr, "A frequency-reconfigurable antenna architecture using dielectric fluids," *IEEE Trans. Antennas Propag.*, vol. 63, no. 12, pp. 5280–5286, Dec. 2015.

[17] S. Wang, L. Zhu, and W. Wu, "A novel frequency-reconfigurable patch antenna using low-loss transformer oil," *IEEE Trans. Antennas Propag.*, vol. 65, no. 12, pp. 7316–7321, Dec. 2017.

[18] J. Liang, G. Huang, K. Qian, S. Zhang, and T. Yuan, "An azimuth-pattern reconfigurable antenna based on water grating reflector," *IEEE Access*, vol. 6, pp. 34804–34811, 2018.

[19] Y. Qian and Q. Chu, "A polarization-reconfigurable water-loaded microstrip antenna," *IEEE Antennas Wireless Propag. Lett.*, vol. 16, pp. 2179–2182, 2017.

[20] A. Singh and C. Saavedra, "A frequency-reconfigurable water-loaded planar monopole antenna," in *Proc. Int. Symp. Antenna Technol. Appl. Electromagn. (ANTEM)*, Waterloo, ON, Canada, Aug. 2018, pp. 1–4.

[21] M. J. Ammann and M. John, "Optimum design of the printed strip monopole," *IEEE Antennas Propag. Mag.*, vol. 47, no. 6, pp. 59–61, Dec. 2005.

[22] D. M. Pozar, *Microwave Engineering*. Hoboken, NJ, USA: Wiley, 2009.

[23] N. D. Pavlov and Y. A. Baloshin, "Electromagnetic properties of water on ghz frequencies for medicine tasks and metamaterial applications," *J. Phys.: Conf. Ser.*, vol. 643, Art. no. 012047, 2015.